

Quasielastic Electron Scattering and a Giant Collective State in $^{209}\text{Bi}^\dagger$

S. Klawansky, H. W. Kendall, and A. K. Kerman

*Laboratory for Nuclear Science, and Department of Physics, Massachusetts Institute of Technology,
Cambridge, Massachusetts,*

and

D. Isabelle*

Laboratoire de L'Accélérateur Linéaire, Orsay, France

(Received 4 October 1972)

Inelastic electron scattering from ^{209}Bi in the momentum transfer range $q = 150\text{--}300\text{ MeV}/c$ induces a broad, strong excitation at about 20 MeV which cannot be explained by shell-model quasielastic knockout calculations. The excitation form factor exhibits a diffraction pattern whose dependence on q is consistent with preliminary predictions for previously unobserved $E0$ or $E2$ giant collective modes in the ^{208}Pb region.

In this paper we summarize experimental data and present a theoretical quasielastic model for the inelastic scattering of electrons from ^{209}Bi .¹ The primary energy k of the electrons was in the range 101–245 MeV, and spectra were taken at several angles, θ , between 67 and 81°, with energy losses, $\nu = k - k'$, up to 144 MeV, where k' is the electron's final energy. In these experiments only the final electrons were detected. The theoretical model uses the nonrelativistic electron-nucleon scattering formalism of McVoy and Van Hove.² For a given θ , ν , and momentum transfer q , we calculate the cross section for knocking the nucleons out of their shell-model bound states. We treat this quasielastic reaction as essentially a free electron-nucleon scattering modified by the momentum distribution and binding energy of the initial state and the distortion of the electron and nucleon scattering wave functions by the heavy nucleus. The quasielastic peak provides direct information on dynamic properties of the nuclear ground state.³

Using reasonable values for the nuclear parameters in our model we obtain relatively good fits to the quasielastic peak. In certain kinematic regions we observe two peaks, only one of which can be identified as the quasielastic peak. No set of nuclear parameters in our model can warp the theoretical quasielastic shape to fit both peaks simultaneously. When we subtract the quasielastic contribution, we are left with a strong nuclear excitation centered around 20 MeV, which is 8 MeV above the expected location of the giant dipole resonance. The giant dipole contribution cannot be resolved in the present data. We have extracted the form factor and find that it exhibits a diffraction pattern as a function of q , which is character-

istic of a collective nuclear excitation. The form-factor strength and shape are consistent with preliminary predictions for $E0$ and $E2$ giant modes in the ^{208}Pb region.^{4, 5}

The experiment was performed at the Laboratoire de l'Accélérateur Lineaire (Orsay, France) in the so-called "250-MeV room." The equipment has been described in detail.^{6, 7} The incident beam had a momentum spread $\Delta p/p = 0.5\%$. The electrons scattered from a ^{209}Bi target (thickness 0.120 g cm^{-2}) were momentum analyzed with a double-focusing spectrometer. A set of tungsten slits located at the focal point limited to 1.1% the momentum bin of the electrons detected in a single Čerenkov Counter. The total energy resolution was 1.6%. The incident beam intensity was measured with a secondary electron monitor⁸ frequently calibrated against a Faraday cup. The absolute normalization of the experimental setup was obtained by measuring the $e-p$ cross section under the same kinematical condition. The statistical accuracy on each measured point was 5%, while the systematic error was of the order of 3%.

Important corrections to the data had to be made to account for radiative effects.⁹ To carry out the corrections it was necessary to measure inelastic cross sections at fixed angles over ranges of both k and k' . 10 values of k in the range 101–245 MeV were employed at $\theta = 81^\circ$, for example, and at each value of k , measurements were made in k' in steps typically in the range 10–15 MeV. Model-independent radiative corrections were applied to the data taken at each angle, including the elastic and inelastic yields, using the formula of Bjorken.¹⁰ Interpolation techniques were used to derive cross sections from the measurements with finer steps in k and k' than those employed in the measure-

ments in order to carry out the corrections. A variety of studies were made to verify that the corrected results were substantially independent of the choices of mesh interval and interpolation procedure. The results presented here are drawn from the body of measured and interpolated corrected results, and the number of points displayed was chosen to represent the amount of measured data available in each region. The use of interpolated points in the displayed data results in a scatter of the points that is less than what would otherwise be expected on the basis of the magnitude of the statistical errors. Systematic uncertainties arising from the radiative correction pro-

cedures are estimated to be about 6%.

Figure 1 shows four spectra at constant θ and q , and the double peaking strongly suggests a low-energy excitation. The quasielastic peak is most visible in the region of $q=250$ MeV/ c and we will fit our model in this region; at lower momentum transfers the low-energy excitation dominates the observed inelastic spectra.

One set of quasielastic calculations was performed in the following manner. We employed a harmonic-oscillator (HO) wave function $u_{nl}(r)$ with binding energy B_{nl} for each initial bound state and a plane wave (PW) of momentum $p=[2M(\nu-B_{nl})]^{1/2}$ for the ejected nucleon. The cross section is then

obtained in closed form (HO-PW):

$$\frac{d\sigma}{d\Omega dk'} = \sum_{\text{orbitals}} \frac{d^2\sigma_{nl}^i}{d\Omega dk'} \quad \left\{ \begin{array}{l} i=1 \text{ for proton} \\ i=2 \text{ for neutron} \end{array} \right. \quad (1)$$

$$\frac{d^2\sigma_{nl}^i}{d\Omega dk'} = f^2(q_\mu^2) \sigma_m [W_{i1} + W_{i2}], \quad (2)$$

$$W_{i1} = \left[\left(1 - \frac{\nu}{M} \right) \delta_{i1} + \frac{K^2 q^2}{4M^2} + \frac{(K + \delta_{i1})^2}{2M^2} \tan^2 \frac{1}{2} \theta \right] S_{nl}, \quad (3)$$

$$S_{nl} = \frac{M}{q} \sum_{m=0}^{n-1} \sum_{j=0}^{n-1-m} C(n, l, m, j) \left[\frac{e^{-p_-^2/\beta}}{(\pi\beta)^{1/2}} \sum_{s=0}^r \frac{r!}{(r-s)!} \left(\frac{p_-^2}{\beta} \right)^{r-s} - \frac{e^{-p_+^2/\beta}}{(\pi\beta)^{1/2}} \sum_{s=0}^r \frac{r!}{(r-s)!} \left(\frac{p_+^2}{\beta} \right)^{r-s} \right], \quad (4)$$

$$C(n, l, m, j) = \frac{(-1)^j 2^j}{m! j! (n-1-m-j)!} \frac{\Gamma((n-1) + l + \frac{3}{2} + m)}{\Gamma(l + \frac{3}{2} + m)} \frac{\Gamma(\frac{3}{2})}{\Gamma(l + 2m + j + \frac{3}{2})}, \quad (5)$$

where $f^2(q_\mu^2)$ is the square of the nucleon elastic form factor as a function of the four-momentum transfer, q_μ^2 , and σ_m is the Mott cross section. K , the average of the absolute magnitudes of the proton and neutron anomalous g factors, is approximately 1.85, and $pM/(2\pi)^3$ is the final nucleon density of states factor. In addition,

$$\begin{aligned} p_+ &= q + p, \\ p_- &= q - p, \\ r &= 2m + j + 1, \end{aligned}$$

β is the oscillator parameter in units of fm^{-2} , $W_{22}=0$, and W_{12} arises from current and spin terms in the Hamiltonian which in the kinematic regions analyzed are an order of magnitude smaller than W_{11} , but were retained in our numerical calculations. The peak position is given approximately by

$$\nu \simeq \frac{q^2}{2M} + \bar{B}_{nl}. \quad (6)$$

The set of orbital binding energies used was consistent with known hole state energies and also with results of Hartree-Fock calculations.^{11, 12}

The average binding energy of the protons from this set was 24 MeV. The protons contributed 85–90% of the cross section at the angles and momentum transfers given.

Figure 2 shows a comparison of experiment with the HO-PW curve. We use one oscillator parameter value, $\beta=0.166 \text{ fm}^{-2}$, for all orbitals. When we integrate the HO-PW doubly differential cross section over all energy loss ν , the result lies within 3–4% of the sum of the free proton and neutron cross sections at the same θ and q . The calculated cross sections exceed the measurements by a factor of more than 2. However, we must take into account the distortion of the electron wave function by the Coulomb field of the heavy nucleus. To do this we use Czyz and Gottfried's recipe¹³ of replacing all electron momentum transfers, \vec{q} , by a momentum transfer, \vec{q}' , given by

$$\vec{q}' = \vec{q} + \frac{3}{2} \frac{Ze^2}{R} (\hat{k} - \hat{k}'), \quad (7)$$

where R is the radius of the spherical charge distribution. In ²⁰⁹Bi, $R \sim 7.1 \text{ fm}$, and with $q \sim 250 \text{ MeV}/c$, $q' \sim 1.1q$, so that the cross section, which

varies as $1/q_\mu^4$, is reduced by about 40%, while the theoretical peak position moves to higher ν . See Fig. 2

To incorporate distortion of the final-state nucleon wave function we assume that the ejected nucleon with final kinetic energy KE sees an energy-dependent nuclear potential of depth V , so that its effective wave number is

$$p' = p \left[1 + \frac{V}{\text{KE}} \right]^{1/2}. \quad (8)$$

We replace p by p' everywhere except in the density of states factor. The use of an energy dependence given by $V = -30 + 0.1 \text{ KE}$ (MeV) reduces the (HO-PW) result by about 30% [harmonic oscillator, effective plane wave (HO-EPW)] at $q = 250 \text{ MeV}/c$. Electron distortion is included in both. See Fig. 2. We note that the location of the (HO-EPW) theoretical quasielastic peak could have been improved by an increase in the average binding energy of 10 MeV.

In our second, more refined treatment of final-state distortion we expand the ejected-nucleon wave function in a partial-wave series and by nu-

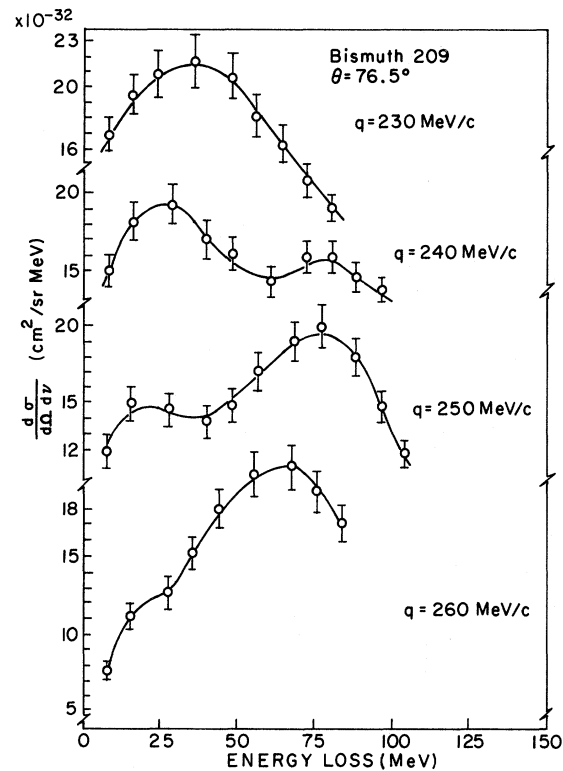


FIG. 1. Inelastic spectra for electrons on ^{209}Bi . $\theta = 76.5^\circ$, $q = 230, 240, 250,$ and $260 \text{ MeV}/c$. The data points are interpolations between measured points. See text for further discussion. Solid curves are visual fits to the points.

merical integration generate continuum wave functions from a real Woods-Saxon optical potential. In this case [harmonic oscillator, distorted wave (HO-DW)], with no spin dependence, we get

$$S_{nl} = \frac{pM}{(2\pi)^3} (4\pi)^2 \sum_{l_1, l_2} (2j+1)(2l+1)(2l_1+1)(2l_2+1) \times \begin{pmatrix} l_1 & l_2 & l \\ 0 & 0 & 0 \end{pmatrix}^2 |F_1(l_2)|^2, \quad (9)$$

$$F_1(l_2) = \int_0^\infty r^2 dr f_{l_1}(p, r) j_{l_2}(qr) u_{nl_j}(r), \quad (10)$$

where $f_{l_1}(p, r)$ is the continuum wave function and the overlap integrals are calculated numerically. The result using the same HO wave functions, $u_{nl_j}(r) \equiv u_{nl}(r)$, a Woods-Saxon optical potential of radius 7.5 fm, diffusivity 0.8 fm, and energy dependence $V = -30 + 0.1 \text{ KE}$ (MeV) is shown in Fig. 2. The discrepancy in peak magnitude and shape between the HO-EPW and the HO-DW calculations shows that the result is sensitive to the choice of final continuum wave function and normalization. We feel that the conventional DW normalization

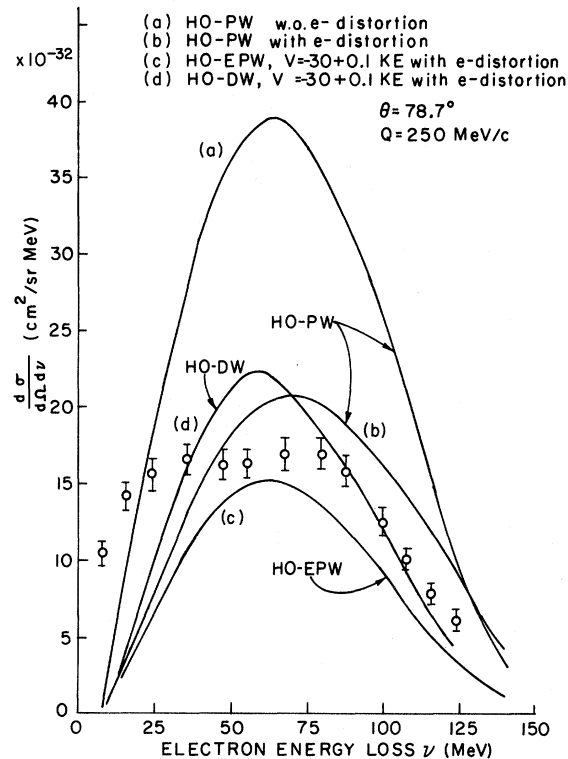


FIG. 2. Experimental points and theoretical curves for $\theta = 78.7^\circ$, $q = 250 \text{ MeV}/c$. (a) HO-PW without electron distortion; (b) HO-PW with electron distortion; (c) HO-EPW, $V = -30 + 0.1 \text{ KE}$ (MeV), with electron distortion; (d) HO-DW, $V = -30 + 0.1 \text{ KE}$ (MeV) with electron distortion. (See text for definition of HO-PW, HO-EPW, and HO-DW.)

to unity amplitude at infinity is not appropriate for the knockout reaction. The scattered electron is only "aware" of having transferred an effective momentum to the struck nucleon within the nuclear well (HO-EPW normalization), and therefore does not carry any information about the continuum nucleon at infinity (HO-DW normalization).

These calculations represent an important improvement¹³⁻¹⁷ over the Fermi-gas models for (e, e') scattering in the ^{208}Pb region for the following reasons: (1) The shell structure of the initial state is incorporated via the bound-state wave functions; (2) the use of orbital binding energies allows a better determination of the rise of the quasielastic cross section at low ν ; (3) improved nucleon continuum wave functions are employed;

(4) the single-particle contributions in the tail region are finite, whereas the Fermi-gas model gives zero cross section beyond a cutoff.

To analyze the low-energy excitation we subtract the quasielastic contribution, σ_{qe} , from each of the constant q spectra, σ_{exp} . We use the (HO-EPW) quasielastic calculation with $V = -30 + 0.1$ KE (MeV) including electron distortion. These choices provide a reasonable fit to the experimental quasielastic peaks in the region of 250 MeV/c. (See Fig. 3.) At an energy ν_0 near the center of the excitation we take a slice of width $\Delta\nu$ and calculate the excitation form factor

$$F^2(\theta, q) = \int_{\nu_0 - \Delta\nu/2}^{\nu_0 + \Delta\nu/2} \frac{[\sigma_{exp}(\theta, q, \nu) - \sigma_{qe}(\theta, q, \nu)]}{Z^2 \sigma_{Mott}(\theta, q, \nu)} d\nu. \quad (11)$$

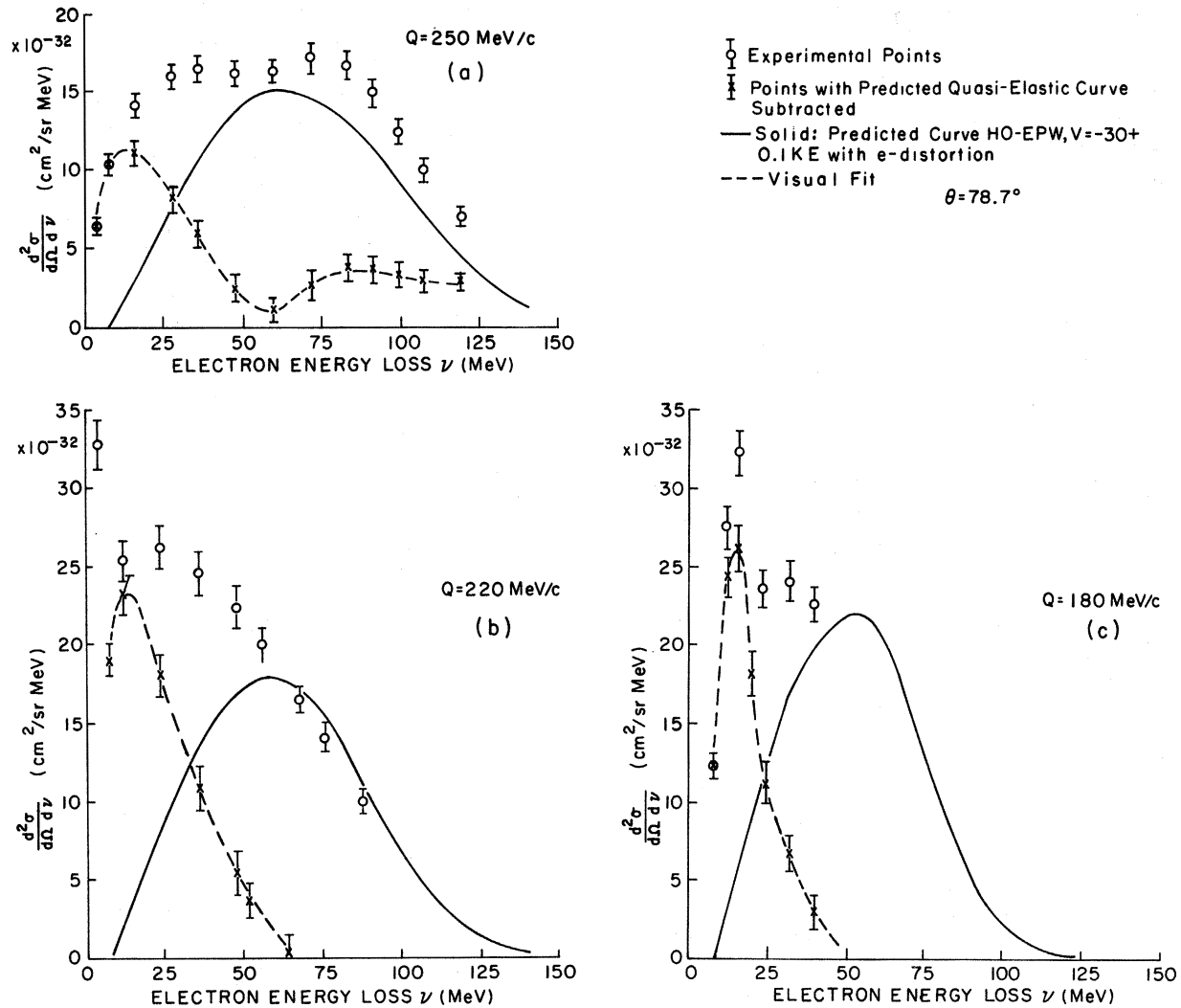


FIG. 3. Experimental points for $\theta = 78.7^\circ$, $q = 250$ (a), 220 (b), and 180 MeV/c (c). The solid line is HO-EPW with $V = -30 + 0.1$ KE (MeV) and electron distortion. The \times 's represent the result of subtracting the HO-EPW result from the experimental data.

If the excitation is in fact a well-defined resonance, $F(\theta, q)$ should depend only on q .

Figure 4 shows the resulting form factors for $\nu_0 = 20$ MeV, an arbitrary slice width, $\Delta\nu = 8$ MeV, and $\theta = 74.3, 76.5, 78.7,$ and 81.0° . Figure 5 shows the results for $\theta = 81.0^\circ$, $\Delta\nu = 8$ MeV, $\nu_0 = 16, 20, 24,$ and 28 MeV. Analysis of the curves shows that the resonance peak lies in the vicinity of 20 MeV.

The fluid oscillation model for the 0^+ or 2^+ state predicts that the form-factor minima will occur at the zeros of $j_l(qR)$.⁴ Fallieros and Deal have used a method based on an energy-weighted sum rule to obtain form factors for the 0^+ and 2^+ collective states in ^{208}Pb which results in essentially the same locations for the diffraction minima.⁵ Table I shows the values of q in units of fm^{-1} for which $j_l(qR) = 0$ when $R = 7.1$ fm. We see that these predictions for the locations of the zeros for 0^+ or 2^+ states are consistent with those observed ex-

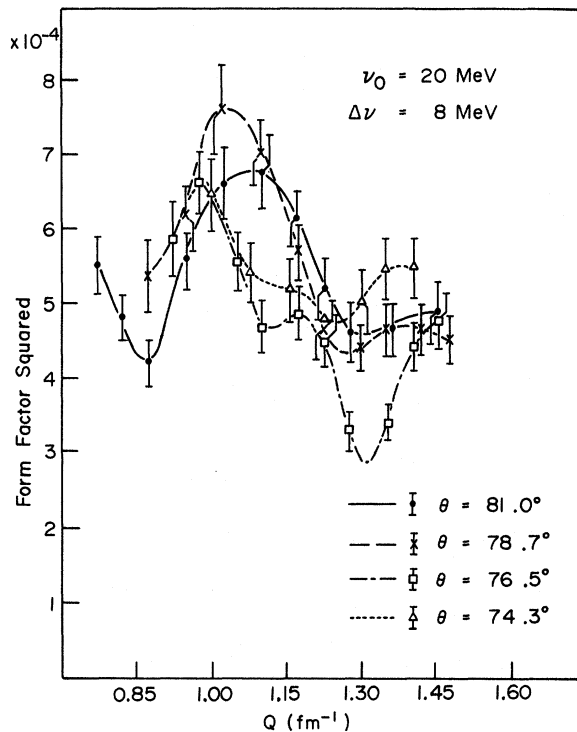


FIG. 4. Excitation form factor squared as a function of q for scattering angles $\theta = 74.3, 76.5, 78.7,$ and 81.0° , obtained by using Eq. (11) with $\nu_0 = 20$ MeV, and $\Delta\nu = 8$ MeV. σ_{qe} is the HO-EPW result with $V = -30 + 0.1$ KE (MeV) and electron distortion. The errors shown are statistical only. The largest contribution to the uncertainties in the form factor arises from uncertainties in the predicted quasielastic distributions. This contribution is not included in the errors shown in the figure but is discussed in the text.

perimentally in ^{209}Bi . We note that the theoretical minima for dipole excitation occur near the observed maxima. The present experiment cannot distinguish between monopole and quadrupole excitation.

Fallieros and Deal find a magnitude of 3×10^{-5} for the second maximum of $F^2(q)$ if they normalize the strength to the long-wavelength limit but expect somewhat larger magnitudes otherwise. This is to be compared with the observed experimental value of about 6×10^{-4} for $\Delta\nu = 8$ MeV. We note that if the optical potential is reduced to $V = -20 + 0.1$ KE, about the largest reduction which still provides a reasonable fit to the quasielastic peak, the quasielastic peak height at $q = 1.05 \text{ fm}^{-1}$ increases by 20%. However, the strength of the observed second maximum, as obtained from Eq. (11) and which occurs at $q = 1.05 \text{ fm}^{-1}$, is decreased by less than 10%.

Although our choice of model parameters optimized the fits to the quasielastic peaks in the vicinity of q about 1.25 fm^{-1} , we are unable to determine whether the fits are equally good in regions below about 1.0 fm^{-1} . The uncertainties in the low-energy excitation yields are dominated by uncertainties that arise from subtraction of

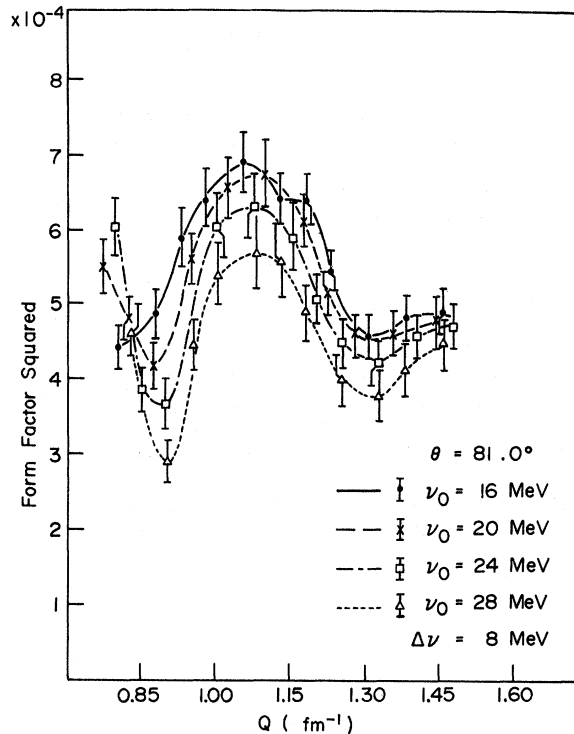


FIG. 5. Excitation form factor squared as a function of q for $\theta = 81.0^\circ$, $\Delta\nu = 8$ MeV, $\nu_0 = 16, 20, 24,$ and 28 MeV. σ_{qe} as in Fig. 4. See caption to Fig. 4 for discussion of the errors.

TABLE I. Values of q in units of fm^{-1} for which $j_l(qR) = 0$ when $R = 7.1 \text{ fm}$.

$l=0$		0.89	1.33	1.77
$l=1$	0.63		1.09	1.53
$l=2$		0.81	1.28	1.73
Observed		0.9	1.3	

the quasielastic spectra from the interpolated measured spectra.

In the region of $q \sim 1.1 \text{ fm}^{-1}$ corresponding to the second maximum, the excitation cross section is the same order of magnitude (Figs. 2 and 3) as the quasielastic peak. The existence of the first maximum below $q = 0.8 \text{ fm}^{-1}$ is suggested in Figs. 4 and 5. We expect that a measurement in the range $q = 0.3\text{--}0.7 \text{ fm}^{-1}$, corresponding to the first maximum, will yield a cross section an order of magnitude greater than the quasielastic cross section.

We believe that the existence of the collective excitation that we observe in this experiment is established in spite of the uncertainties arising from the quasielastic subtraction. Additional measurements of inelastic spectra, especially at lower q , would help to determine its width

and define its multipolarity. We note that real photon excitation could only excite the $E2$ state.

In the spectra of electrons scattered inelastically from a heavy nucleus, the high-energy-loss tail is expected to provide information on ground-state nucleon-nucleon correlations.¹³ The observed cross sections for $\nu > 100 \text{ MeV}$ tend to be larger and fall less rapidly than do the theoretical quasielastic curves, suggesting possible evidence of ground-state correlations.

Note added in proof: Fukuda and Torizuka¹⁸ have reported a giant resonance around 28 MeV in ^{90}Zr as well as a resonance in ^{208}Pb which appear to correspond to the state observed in ^{209}Bi .

ACKNOWLEDGMENTS

We would like to thank Stavros Fallieros for his illuminating discussions on theoretical aspects of this problem. We are very grateful to Mrs. Elaine Miller for her help with the analysis. We wish to thank Kurt Gottfried, J. D. Bjorken, John Negele, and Gerry Miller for helpful discussions. We are grateful for help and support from George Bishop, M.-M. Bébin, C. Betourné, and P. Roy during the course of the experiment.

†Work supported in part through funds provided by the Atomic Energy Commission under Contract No. AT(11-1)-3069.

*Permanent address: Laboratoire de Physique Corpusculaire, Université de Clermont, 34 avenue Carnot 63-Clermont-Ferrand, France.

¹D. Isabelle and H. W. Kendall, *Bull. Am. Phys. Soc.* **9**, 95 (1964).

²K. W. McVoy and L. Van Hove, *Phys. Rev.* **125**, 1034 (1962).

³J. D. Walecka, in *High Energy Physics and Nuclear Structure*, edited by S. Devons (Plenum, New York, 1970), p. 1.

⁴T. de Forest and J. D. Walecka, *Advan. Phys.* **15**, 1 (1966).

⁵S. Fallieros and T. Deal, private communication.

⁶F. Lacoste and G. R. Bishop, *Nucl. Phys.* **26**, 511 (1961).

⁷B. Milman, *Onde Electrique* **421**, 22 (1962).

⁸D. Isabelle, *Onde Electrique* **421**, 66 (1962).

⁹H. W. Kendall and D. Isabelle, *Bull. Am. Phys. Soc.* **9**, 95 (1964).

¹⁰J. D. Bjorken, *Ann. Phys. (N.Y.)* **24**, 201 (1963).

¹¹K. S. Masterson and A. M. Lockett, *Phys. Rev.* **129**, 776 (1963).

¹²J. W. Negele, *Phys. Rev. C* **1**, 1260 (1970).

¹³W. Czyz and K. Gottfried, *Ann. Phys. (N.Y.)* **21**, 47 (1963).

¹⁴W. Czyz, *Phys. Rev.* **131**, 2141 (1963).

¹⁵E. J. Moniz, I. Sick, R. R. Whitney, J. R. Ficenece, R. D. Kephart, and W. P. Trower, Stanford Report No. ITP-377, 1971 (to be published).

¹⁶T. de Forest, Jr., *Nucl. Phys.* **A132**, 305 (1969).

¹⁷T. W. Donnelly, *Nucl. Phys.* **A150**, 393 (1970).

¹⁸S. Fukuda and Y. Torizuka, *Phys. Rev. Letters* **29**, 1109 (1972).